Minielectrode catheter technology for near zero-fluoroscopy substrate-guided ablation of typical atrial flutter

Johanna Betz, MD,[*1] Laura Vitali-Serdoz, MD,[†1] Veronica Buia, MD,[†] Janusch Walaschek, MD,[†] Harald Rittger, MD,[†] Dirk Bastian, MD[†]

*From the *Faculty of Medicine, Friedrich-Alexander-University Erlangen-Nuernberg (FAU), Erlangen, Germany, and [†]Department for Cardiology, Klinikum Fuerth, Teaching Hospital of Erlangen-Nuernberg University, Fuerth, Germany.*

BACKGROUND MicroFidelity catheter technology may facilitate voltage-guided ablation by high-resolution electroanatomic mapping (HR-EAM) and precisely targeted energy application.

OBJECTIVE To evaluate the performance of minielectrode (ME) technology for zero-fluoroscopy substrate-guided cavotricuspid isthmus (CTI) ablation.

METHODS Eighty-two patients underwent near zero-fluoroscopy substrate-guided CTI ablation using a nonirrigated large-tip catheter with 3 MEs. The CTI was subdivided into 15 electroanatomic segments. Bipolar voltage maps were compared with ME signals. The outcome was compared with a historic cohort of 92 patients who underwent linear ablation.

RESULTS Compared with linear ablation, the substrate-guided approach was associated with an almost halved ablation duration (336 ± 228 vs 649 ± 409 seconds, $P < .001$), halved radiofrequency energy applied (14.2 ± 10.6 vs 28.6 ± 19.6 kJ, $P < .001$), and shorter procedure duration (60.8 ± 33.8 vs 76.3 ± 40.9 minutes, $P = .008$) limiting the extent of energy delivery to 22.7% of the CTI area. HR-EAM visualized 2.03 ± 0.88 conductive pathways with a diameter of 5.35 ± 1.98 mm. A higher number of ME-detected bundles and a larger channel diameter correlated with increased ablation requirements. In 97.6% of the voltage-guided and 88.0% of the linear procedures, fluoroscopy was not used.

CONCLUSION HR-EAM-based substrate-guided CTI ablation may improve procedural outcome compared with the linear approach. Enhanced identification of discrete conductive pathways correlates with ablation efficacy. The electroanatomic subdivision of the CTI into 15 segments was feasible and may improve the understanding and comparability of anatomic variants and ablation results. Independent of the ablation strategy, modern EAM technology enables safe zero-fluoroscopy procedures in the majority of cases.

KEYWORDS Atrial flutter; Catheter ablation; Electroanatomic mapping; Maximum voltage-guided; Zero fluoroscopy

(Heart Rhythm O^2 2021;2:262–270)

Introduction

Radiofrequency catheter ablation of the cavotricuspid isthmus (CTI) represents the first-line treatment for typical atrial flutter (AFL).[1–4] Although its efficacy is high, the conventional ablation is still time-consuming and requires a considerable amount of radiation,[5] and treatment failure occurs.[6–8]

The maximum voltage (MV)-guided (MVG) approach aims to identify and selectively ablate conductive muscle fibers. Therefore, accurate identification of MV areas and precisely targeted radiofrequency energy (RFE) application are decisive factors. Although a reduction of ablation requirements has been shown,[9–13] the current evidence is still considered to not be robust enough to suggest a general change in the ablation strategy.[14] In addition, there are conflicting data regarding fluoroscopy time (FT).[9,11]

MicroFidelity sensor technology (Boston Scientific, North Quincy, MA) was developed to enhance spatial resolution of large-tip catheters using 3 minielectrodes (ME) with a diameter of 1.2 mm radially integrated into the distal tip. By reducing the gap between the origin of high-resolution (HR) signals and the center of RFE application, this technology may facilitate MVG ablation.[15] The goal of this study was to evaluate the procedural performance of the ME for zero-fluoroscopy substrate-guided CTI ablation.

Methods

Study population

Two-hundred ninety consecutive patients underwent CTI ablation for documented typical AFL between June 2016

[1]The first 2 authors contributed equally to the study and the manuscript.

Address reprint requests and correspondence: Ms Johanna Betz, Klinikum Fürth, Jacob-Henle-Str. 1, 90766 Fürth, Germany. E-mail address: betz.johanna@gmx.net.

2666-5018/

https://doi.org/10.1016/j.hroo.2021.03.010

KEY FINDINGS

- Minielectrode-based high-resolution electroanatomic mapping (EAM) of the cavotricuspid isthmus (CTI) significantly improves identification of crucial conductive pathways correlating with ablation efficacy.
- A stepwise substrate-guided approach using modern AutoMap features may reduce procedure duration by obviating repeat mapping and almost halves ablation time and applied energy compared with linear ablation.
- Standardized subdivision of the CTI into 15 segments may support the understanding and comparability of its electroanatomy.
- Independent of the treatment strategy, modern EAM enables safe fluoroless CTI ablation in the majority of procedures.

and October 2019. All patients provided informed consent for the intervention and data documentation. The study was performed according to the requirements for obtaining the medical degree (Dr med.), is approved by the responsible ethics committee, adhered to the Declaration of Helsinki, and is registered at the German Registry for Clinical Trials (DRKS00020533). Patients with implanted cardiac devices (n = 21), previous CTI ablation (n = 18), nonconvertible atrial fibrillation (n = 1), concomitant pulmonary vein isolation (n = 43), and a different catheter setting (n = 33) were excluded from this analysis. Therefore, study group 1 consisted of 82 prospectively enrolled patients undergoing MVG ablation using the ME catheter since September 2017 and was compared to a historic group of 92 patients treated with conventional linear CTI ablation between June 2016 and November 2018 (group 2). These groups were not different regarding baseline characteristics (Table 1).

Electrophysiological study

Two decapolar catheters were each positioned in the coronary sinus and along the tricuspid valve annulus (TVA). A 3-dimensional electroanatomic mapping (EAM) system (EnSite Velocity™, since 2018 Precision™; Abbott, St Paul, MN) was used for catheter positioning, mapping, and ablation in all procedures. Mapping and ablation were conducted either during ongoing flutter or, when presenting in sinus rhythm, during pacing from the proximal coronary sinus.

Group 1: MVG/ME

The MVG approach was performed using the nonirrigated 8-mm IntellaTip MiFi XP™ catheter (Boston Scientific). Both conventional distal bipolar (CDB) signals and bipolar electrograms from all ME were recorded simultaneously along the inferior CTI using the EnSite AutoMap module (Figure 1). Local peak-to-peak amplitudes were visualized in a bipolar voltage map first (point border interpolation 5–7). Besides tagging the point of MV, color-coding was set to mark areas with ≥70% of the measured MV as conductive bundles initially. The color threshold could be adapted according to the individual voltage characteristics for best bundle identification. Thereafter, a second voltage map was created using the EnSite TurboMap feature for automated analysis of the ME signals deriving from the original mapping dataset at 10× real-time speed. The CTI was subdivided into 15 sections as shown in Figure 1. Following a stepwise voltage-guided approach, RFE (60 W/60°C) was applied for 20–60 seconds according to the local amplitude reduction,[13,16] beginning at the point of MV recorded by ME mapping, and continued at areas with ≥70% of the measured MV. If no bidirectional conduction block (BCB) was achieved, the voltage border was gradually reduced to identify adjacent areas with higher voltage, possibly representing larger conduction channels. Further, RFE was applied at these spots. In case of continued inefficacy, a re-map was performed and RFE delivery was extended to sites showing residual slow conduction. Ultimately, the operator could proceed to linear ablation.

Group 2: Conventional approach

Patients in group 2 underwent standard EAM-guided linear CTI ablation as described elsewhere in detail.[1,17] The nonirrigated 8-mm-tip catheter RF-Contactr™ (Medtronic, Minneapolis, MN) and Therapy™ (large or X-large curve; Abbott) were used for temperature-controlled ablation (50–60 W, 50–60°C) in 56 (61%) and 36 patients (39%), respectively. The procedural endpoint for both groups was BCB with established characteristics,[3] persisting after a waiting period of 30 minutes.

Follow-up

All patients underwent postinterventional echocardiography and telemetric monitoring for 24 hours. Clinical follow-up including Holter monitoring was performed by the outpatient clinic or the referring cardiologist.

Statistical analysis

A minimum sample size of 59 patients per group was required to detect a 35% difference in cumulative ablation

Table 1 Baseline characteristics of the study patients according to procedural approach

Variable	Linear n = 92	MVG/ME n = 82	*P* value
Male	54 (58.7 %)	55 (67.1%)	.254
Age (years)	67.71 ± 12.21	68.50 ± 10.97	.654
BMI (kg/m^2)	27.08 ± 4.85	27.98 ± 5.06	.234
Area right atrium (cm^2)	18.66 ± 4.15	19.08 ± 4.04	.523
Area left atrium (cm^2)	22.16 ± 5.04	21.58 ± 5.05	.457
Ejection fraction (%)	64.22 ± 11.83	62.01 ± 11.58	.217
Atrial fibrillation	48 (52.2%)	41 (51.2%)	.904
Arterial hypertension	60 (65.2%)	61 (75.3%)	.149
Diabetes mellitus	18 (19.6%)	14 (17.1%)	.672

BMI = body mass index; ME = minielectrode; MVG = maximum voltage-guided.

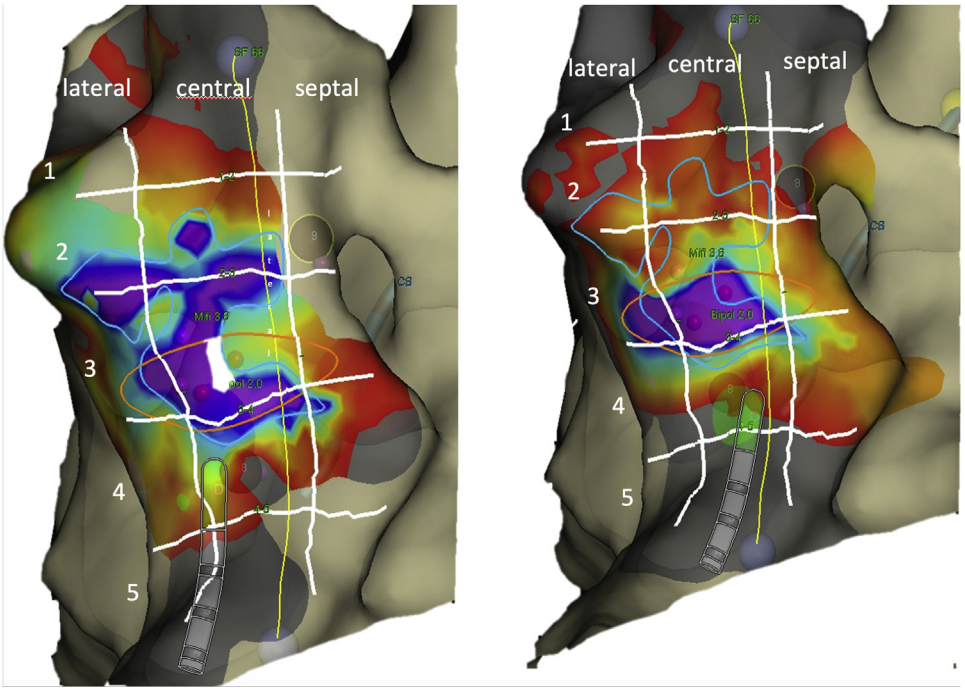

Figure 1 EnSite Precision (Abbott, St Paul, MN) cavotricuspid isthmus (CTI) voltage map (caudal view, 6 o'clock). **Left:** Minielectrodes (Turbo map; 255 points); **Right:** Conventional bipolar signals (196 points). Visual electroanatomical classification of the CTI into 3 longitudinal levels (inferolateral, central, and paraseptal isthmus) and 5 transversal segments (from 1 = anterior myocardial vestibule near tricuspid valve annulus to 5 = posterior membranous sector adjacent to the Eustachian valve and inferior vena cava). Purple indicates a local amplitude ≥70% of the individual maximum CTI voltage. The bipolar map on the right shows a single high-voltage bundle (segments C3/L3). Ablating this site did not delay local conduction. The minielectrode map (left) visualized much better the complex architecture showing 2 parallel conducting bundles and an additional oblique connection. Energy delivery at the oblique bundle delayed local conduction. Additional ablation at the second inferoseptal exit (segment S2) resulted in bidirectional conduction block (total ablation time 260 seconds). Yellow line = CTI length.

duration between both ablation strategies (main hypothesis) with a statistical power of 90% at a 2-sided 5% significance level, including an addition of 15% owing to planned use of a nonparametric test. Results are presented as means ± standard deviation or median and interquartile range. Continuous variables were compared by unpaired *t* test or Mann–Whitney *U* test for normally and non-normally distributed data, respectively. The χ^2 test or Fisher exact test was used for nominal variables. Correlation of continuous variables was assessed by Pearson correlation coefficient. A *P* value < .05 was considered statistically significant.

Results

Procedural outcome

Procedural outcome is shown in Table 2. Acute success was achieved in 80 patients (97.6%) undergoing MVG ablation and in 87 patients (94.6%) in group 2 (P = .449).

Compared with the linear approach, voltage-guiding significantly reduced ablation duration (336 ± 228 vs 649 ± 409 seconds, –48.2%, *P* < .001, Figure 2), RFE (14.24 ± 10.58 vs 28.58 ± 19.58 kJ, –50.2%, *P* < .001), and the number of ablation points (7.82 ± 6.08 vs 11.38 ± 9.79, –31.3%, *P* = .010). Additional ablation owing to acute

Table 2 Procedural outcome according to ablation strategy

Variable	Linear n = 92	MVG/ME n = 82	*P* value
Acute ablation success	87 (94.6%)	80 (97.6%)	.449
Cumulative ablation duration (s)	649 ± 409	336 ± 228	<.001
Radiofrequency energy (kJ)	28.58 ± 19.58	14.24 ± 10.58	<.001
Number of ablation points	11.38 ± 9.79	7.82 ± 6.08	.010
Procedure duration (min)	76.3 ± 40.9	60.8 ± 33.8	.008
Minor complications, total	5 (5.4%)	4 (4.9%)	1.000
Groin hematoma	2 (2.2%)	4 (4.9%)	.423
Pop phenomenon	2 (2.2%)	0	.499
Agitation under sedation	1 (1.1%)	0	1.000
Zero-fluoroscopy procedures	81 (88.0%)	80 (97.6%)	.011
Fluoroscopy time (min)	0.3 ± 1.2	0.1 ± 1.2	.018
Effective dose (μSv)	12.21 ± 50.81	2.59 ± 23.30	.010

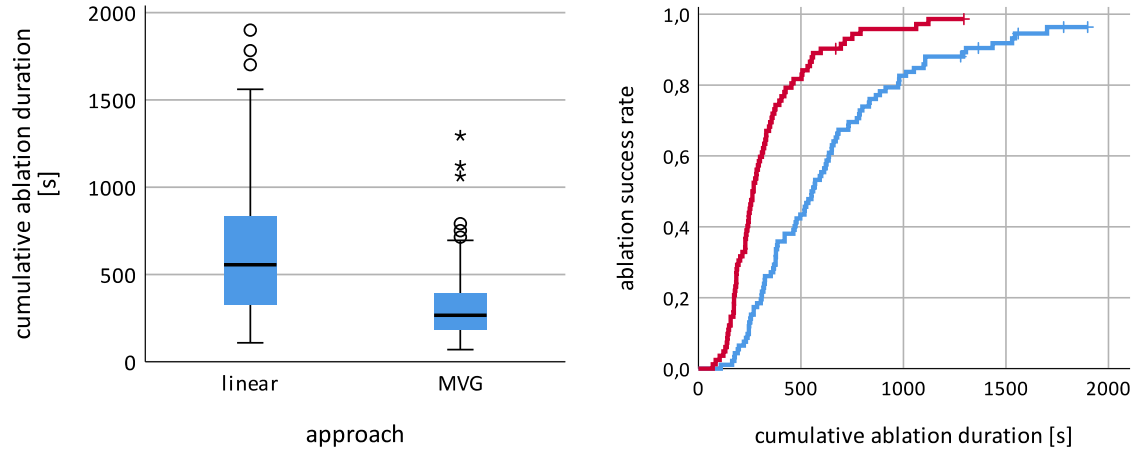

Figure 2 Ablation duration according to treatment. **Left:** Ablation time according to ablation strategy; **Right:** Ablation success rate with red = group 1 (maximum voltage-guided [MVG] / minielectrode), blue = group 2 (conventional linear).

reconnection during the waiting period was needed in 13 cases of the MVG group (15.9%) compared with 8 patients undergoing linear ablation (8.7%; $P = .148$). Four patients from group 1 (4.9%) required complete linear ablation, resulting in BCB in 2 of them. Despite requiring additional time of 8.1 ± 7.0 minutes for voltage mapping, the procedure duration was shorter in the MVG/ME group (60.8 ± 33.8 minutes vs 76.3 ± 40.9 minutes, –20.3%, $P = .008$).

No major complications occurred. Nine minor adverse events were documented (Table 2).

Radiation exposure

A total of 161 procedures (92.5%) were performed without fluoroscopy (97.6% MVG, 88.0% linear), as shown in Table 2. The rate of minor complications was not different between fluoroless ablation (3.7%) and procedures requiring minimal fluoroscopy (7.7%, $P = .425$).

High-resolution voltage-guiding

Data for CDB and ME maps derive from 407 ± 280 and 1209 ± 1027 collected CTI points, respectively. In general, the local MV measured with the ME was higher compared with bipolar signals (9.1 ± 3.4 vs 4.3 ± 2.2 mV, $P < .001$). High-voltage areas (HVA, ≥70% of MV) were found predominantly in central segment C3, followed by C2/4, for both CDB and ME signals (Table 3). ME-based EAM visualized a mean of 2.03 ± 0.88 conductive routes with a diameter of 5.35 ± 1.98 mm compared with 1.41 ± 0.53 pathways for CDB mapping.

In total, 209 ablation points were documented, with the majority set in section C3 (n = 42, 20.1% of all documented ablation points), followed by section C4 (n = 33, 15.8%). The fewest points were applied in the septal column and near the TVA (Table 3).

For ME-based mapping, a higher MV correlated with lower RFE for BCB (r = –0.265, $P = .041$). A higher number of ME-detected conducting pathways and a larger channel diameter correlated with increased RFE, ablation duration, and number of ablation points to BCB. No correlation was found for CDB-detected channels (Table 4; Figure 3).

Voltage guiding enabled to achieve a BCB with RFE delivery at only 22.7% of the entire CTI area (3.4 sections

Table 3 Electroanatomic mapping of the cavotricuspid isthmus (15 segments)

	Segment	Lateral	Central	Septal	Sum
Distribution (%) of high-voltage locations[†]					
CDB map	1	1.5	2.0	0.5	4.0
	2	5.5	11.9	3.5	20.9
	3	11.4	18.4	7.0	36.8
	4	8.0	12.9	4.0	24.9
	5	3.5	8.5	1.5	13.4
	Sum	29.9	53.7	16.4	
HR-ME map	1	0.5	2.5	0.5	3.5
	2	6.4	12.9	4.5	23.8
	3	8.4	18.3	5.4	32.2
	4	7.4	14.9	4.0	26.2
	5	4.5	9.9	0.0	14.4
	Sum	27.2	58.4	14.4	
Distribution (%) of ablation points					
	1	1.0	2.9	1.0	4.8
	2	5.7	13.9	1.4	21.1
	3	10.0	20.1	3.3	33.5
	4	10.5	15.8	1.0	27.3
	5	3.3	10.0	0.0	13.4
	Sum	30.6	62.7	6.7	
Distribution (%) of block points					
	1	1.5	2.9	1.5	5.9
	2	4.4	16.2	1.5	22.1
	3	7.4	16.2	1.5	25.0
	4	7.4	23.5	1.5	32.4
	5	1.5	13.2	0.0	14.7
	Sum	22.1	72.1	5.9	

All figures shown in this table are rounded, so minor discrepancies may arise from addition of these amounts.

CDB = conventional distal bipolar; HR-ME = high-resolution minielectrode.

[†]≥70% of individual maximum voltage.

Table 4 Electroanatomic mapping–detected conductive pathways: Correlation with procedural parameters

	Conductive channels, conventional bipolar signals	Conductive channels, minielectrode signals	Mean diameter of minielectrode-detected channels
Cumulative RFE	r = 0.219, P = .089	r = 0.292, P = .022	r = 0.884, P < .001
Ablation duration	r = 0.206, P = .112	r = 0.315, P = .013	r = 0.866, P < .001
Number of ablation points	r = 0.147, P = .257	r = 0.261, P = .042	r = 0.802, P < .001

RFE = radiofrequency energy.

ablated per patient). The location of the ablation points leading to BCB is shown in Table 3.

Follow-up

During a median follow-up of 12 months (interquartile range 0.5–34.9 months), there were 8 clinical recurrences of CTI-dependent AFL in the linear group (8.7%) after a median time of 101 days between ablation and recurrent flutter compared with 4 patients (4.9%, 98.5 days) after MVG ablation (P = .381). In all patients CTI reconduction was confirmed and reablated successfully.

Seventeen patients without clinical AFL recurrence (11 linear, 6 MVG) underwent a second electrophysiological study for atrial fibrillation ablation. Recurrent CTI conduction was documented and reablated in 2 patients of the linear group (18%) and 1 patient (17%) after MVG ablation (P = not significant).

Discussion

Main findings

Main findings were as follows: (1) Substrate evaluation and identification of discrete conductive pathways may be significantly improved by ME-based HR-EAM and is correlated with ablation efficacy. (2) Using full-automated EAM features for precise ME-guided substrate ablation reduces procedure duration and almost halves ablation time, as well as applied energy, compared with linear ablation. (3) Together with high-resolution mapping, electroanatomic subdivision of the CTI into 15 segments may support the understanding and comparability of individual electroanatomic characteristics. This may further improve the results of targeted ablation. (4) Independent of the ablation strategy, modern EAM enables safe zero-fluoroscopy CTI ablation in the majority of procedures.

Electroanatomic CTI classification

For anatomic description, the CTI has been subdivided into 3 parallel levels, namely, a central inferior, paraseptal, and inferolateral isthmus.[18] In the posterior–anterior direction, the anterior myocardial vestibule near the TVA is distinguished from a middle trabeculated part and a posterior membranous sector. We introduced an electroanatomic subdivision of the CTI into 15 segments with 5 central sectors corresponding to the inferior isthmus bordered by 5 paraseptal and 5 inferolateral segments (Figure 1). The simple visual segmentation could be easily estimated and used by the operator while performing the procedure. For CTI ablation based on the individual electroanatomy aiming for limited and precisely targeted energy application, the approximative CTI segmentation was found to be feasible and helpful, allowing standardized description and comparison of both mapping and ablation results.

Automated EAM for individual substrate-guided ablation

The CTI exhibits a unique but variable architecture of muscular bundles separated by intervening connective tissue.[18] The MVG approach directly targets muscle bundles identified by local high-voltage electrograms. Reproduced by many other working groups,[9,13,19] the concept was proven by Gula and colleagues[11,20] in 2006 and 2009, showing a significant reduction of ablation requirements for the MVG approach compared with linear ablation. However, no correlation was found between the initial CTI voltage and ablation

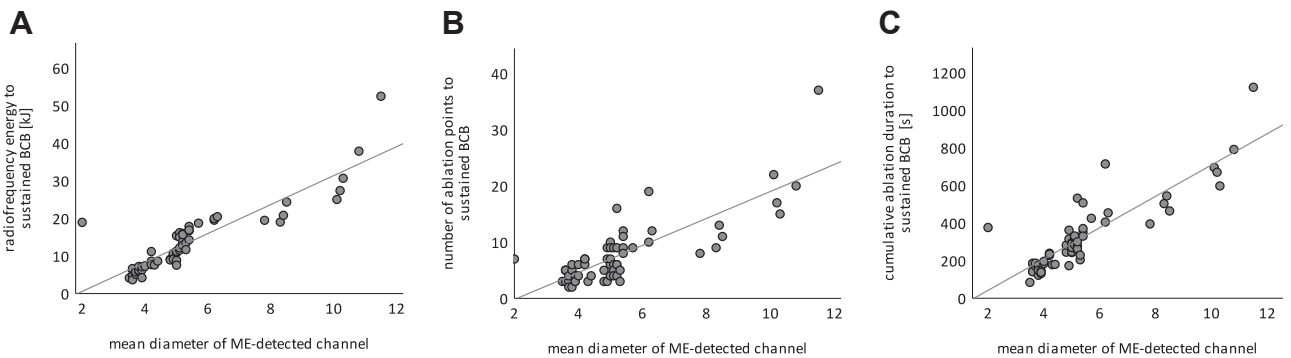

Figure 3 Correlation between the mean diameter of conductive cavotricuspid isthmus pathways detected by minielectrode (ME)-based electroanatomic mapping and ablation parameters (n = 61).

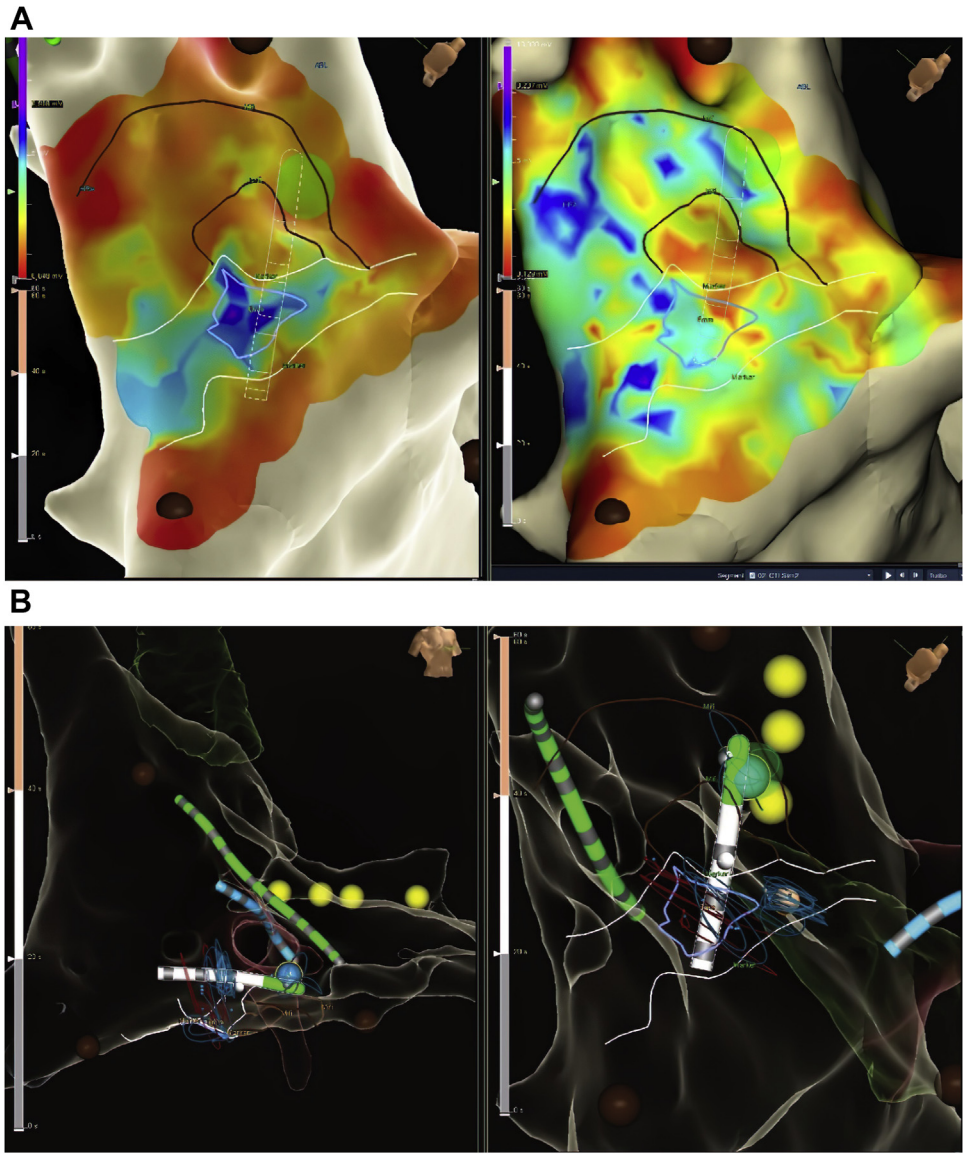

Figure 4 Voltage-guided ablation, complex cavotricuspid isthmus (CTI) electroanatomy, zero-fluoroscopy. **A:** EnSite Precision (Abbott, St Paul, MN) map during CTI-dependent atrial flutter, caudal view, 6 o'clock. Left: conventional bipolar voltage-AutoMap showing a single conduction pathway (*white borders*) with a central high-voltage area of 8 mm^2 (segments C3/4, maximum voltage [MV] 7 mV, blue borders). Right: Minielectrode-TurboMap showing an additional conductive bundle in the more anterior segments 2 (MV 8.2 mV, black borders) and the bundle connection. **B:** Treatment: Initial ablation of the central bundle prolonged the cycle length and terminated the flutter but without bidirectional conduction block (BCB). Successively targeting the anterior pathway resulted in BCB (*turquoise dot*). Left: right anterior oblique view; right: caudal view, 6 o'clock. Yellow dots = His bundle; inferior brown dots = CTI length; cranial brown dot = patent foramen ovale.

requirements that could be explained by less effective lesions applied at previously ablated sites. Without using nonfluoroscopic EAM, the mapping strategy was continuous signal amplitude measurement during initial pull-back, to note and to ablate the site with MV, followed by remapping and further targeting the remaining MV. The additional time needed for repeated mapping prior to each ablation prevented further reduction of procedure duration and FT (86 ± 50 vs 92 ± 53 minutes and 25 ± 14 vs 23 ± 13 minutes for MVG vs linear ablation, respectively).

In contrast to previous strategies, our mapping approach aimed not only to note and target the maximum voltage, but to characterize the individual native CTI electroanatomy and to identify distinct conduction routes as ablation targets based on native HR signals. With respect to the interindividual variations in the CTI anatomy and voltage, we used all signals showing a threshold of ≥70% of the detected individual MV for initial electroanatomic assessment both in the conventional bipolar and the ME maps instead of a fixed general cut-off for measured voltage, as used by Sato and colleagues.[19] In cases with large uniform HVA or no demarcation of bundles, the initial threshold was gradually modified to improve bundle visualization. An advantage of this approach is the individually adopted initial assessment

of the native electroanatomy before changing signal characteristics by ablation, thus avoiding repeated mapping and assessment of altered signals. The strategy was helpful in particular in cases with complex anatomy when the first RFE applications failed to block. Consequently, in this study, the almost halved ablation time achieved by MVG ablation could be translated into a significant reduction in procedure duration.

ME-based CTI mapping for bundle identification

The ME technology was developed to improve the spatial mapping resolution of large-tip catheters.[15,21]

To the best of our knowledge, we evaluated the largest population so far of patients undergoing zero-fluoroscopy MVG ablation based on ME 8-mm-tip catheter mapping, providing comprehensive data on intra- and interindividual comparisons of simultaneously recorded conventional bipolar and ME signals.

Besides showing signals with higher amplitude and sharper configuration, the increased spatial resolution of the ME, together with an individualized EAM approach, allowed direct visualization and differentiation of distinct conductive pathways (Figure 4).

Of course, it is important to note that the distance measured for conductive routes in the voltage map is not necessarily equal to the diameter of anatomical bundles and may vary depending on the mapping settings used. However, using the investigated mapping approach, it was possible to visualize even distinct oblique conductive pathways connecting other bundles, explaining the observed phenomenon of central ablations failing to achieve BCB despite effective RFE delivery and local signal amplitude reduction (Figures 1 and 4). For the first time, we were able to demonstrate a linear correlation of the CTI electroanatomy detected by ME signals with ablation parameters (Figure 3), hereby proving the clinical feasibility of substrate-focused CTI ablation.

It has been shown that ME may be helpful to avoid unnecessary ablation, especially at the annular part of the CTI.[22] This seems to be in contrast to anatomic studies showing thickest bundles in the anterior segments[18] and to findings from Shah[23] demonstrating relevant gaps near the TVA. In our study, careful EAM found a local voltage of $\geq$70% MV in the anterior segments in $\leq$4% for both CDB and ME signals (Table 3). Targeting HVA first, ablation near the TVA was needed only in 4.8%. A possible explanation may be the anatomical course of oblique or longitudinal muscle bundles passing from the middle to the anterior segments terminating on the hinge of the TVA.[18] These anatomic bundles must not be necessarily essential for CTI conduction and—if conductive—may often be effectively ablated in the middle sector when using the MVG approach.

In accordance with Tzeis and colleagues,[15] we found ME mapping useful and superior to CDB signals for assessing the proximal sections near the IVC. Ablation of a muscular Eustachian ridge was needed in 8 patients of the MVG group (13.1%), corresponding to 13.4% of the ablation points applicated.

In an important comment, Caldwell and colleagues[24] stressed occasional difficulties in achieving BCB using the conventional approach of repeated remapping during pullback following RFE application, based on the fact that ME mapping guides the ablation focus more proximal compared with conventional bipolar electrodes. In our study, we also did experience an improved ablation efficacy when placing the large tip of the MiFi XP catheter about 2 mm more distal, following the idea of better covering the bundle displayed by the ME signals and improving tissue contact.

Zero-fluoroscopy CTI ablation

Mol and colleagues[25] suggested using ME to avoid a 3-dimensional navigation system. The approach was associated with a fluoroscopy duration of 18 minutes. On the other hand, there is growing evidence that modern mapping technology and targeted strategies allow for significant reductions of FT.[22,26,27]

Deutsch and colleagues[9] reported a non-fluoroscopy approach for 91% and 93% of the patients undergoing MVG or linear ablation. The results from our study reproduce these findings, showing a zero-fluoroscopy rate of 92.5% irrespective of the ablation strategy. Thirteen of 174 procedures required an FT of 0.3 $\pm$ 1.2 minutes in the linear and 0.1 $\pm$ 1.2 minutes in the MVG group, which is nearly identical to the findings from Deutsch and colleagues. The maximum effective dose was 0.34 mSv in our study and, therefore, lower than 1 mSv in every case matching the definition of near-to-zero fluoroscopy.[28] It is important to underline that the consequent avoidance of radiation was not associated with a higher complication rate.

Limitations

To the best of our knowledge, the study evaluated the largest number of consecutive patients prospectively enrolled to undergo zero-fluoroscopy voltage-guided CTI ablation based on ME EAM so far. The compared groups were not different in relevant clinical characteristics. The sample size provides a sufficient power of over 90% for proving the main hypothesis. However, because the study is limited by the nonrandomized character of a single-center evaluation comparing a new technology with a historic population, the outcome of voltage-guiding is undergoing validation in an ongoing randomized study (Zero MAGIC, NCT04678258).

The ME technology was evaluated by intraindividual comparison with bipolar signals only within the MVG group. The results are encouraging, showing a superior visualization of conductive routes and a significant correlation with ablation requirements for ME mapping. Consequently, the question whether the use of minielectrodes provides any incremental benefit to improve the success rate of voltage-guided procedures should be evaluated further in a prospective randomized controlled trial.

The follow-up was not exactly predefined and is, therefore, limited. Although clinical follow-up was not different between the groups, targeted MVG ablation theoretically may encompass an increased risk for clinically inapparent reconduction. A prospective study with predefined invasive reevaluation of persistent BCB is currently evaluating this issue.

Conclusion

Substrate-guided CTI ablation, using modern AutoMap features, reduces procedure duration by obviating the need for repeat mapping and almost halves ablation time and applied energy compared with linear ablation. Individualized high-resolution mapping significantly improves identification of discrete conductive bundles. A higher number of ME-detected conducting pathways and a larger channel diameter correlates with increased ablation requirements. Standardized subdivision of the CTI into 15 segments may support the understanding and comparability of its electroanatomy. Independent of the treatment strategy, modern EAM technology enables fast, effective, and safe ablation without the need for fluoroscopic control in the majority of cases.

Acknowledgments

We would like to thank Mrs Stefanie List, Mr Dominik Scheller, and Mr Mathias Diester from Abbott for their qualified technical assistance during the procedures. Further, we thank Ms Angela Cruz for language editing and Mr Lukas Kagermeier for support in graphic design.

Funding Sources

This research did not receive any specific grant from funding agencies in the public, commercial, or not-for-profit sectors.

Disclosures

The authors have no conflicts to disclose.

Authorship

All authors attest they meet the current ICMJE criteria for authorship.

Patient Consent

All patients provided informed consent for the intervention and data documentation.

Ethics Statement

The study was approved by the responsible ethics committee, adhered to the Declaration of Helsinki, and is registered at the German Clinical Trials Register.

References

1. Cosio FG, Lopez-Gil M, Goicolea A, Arribas F, Barroso JL. Radiofrequency ablation of the inferior vena cava-tricuspid valve isthmus in common atrial flutter. Am J Cardiol 1993;71:705–709.
2. Natale A, Newby KH, Pisano E, et al. Prospective randomized comparison of antiarrhythmic therapy versus first-line radiofrequency ablation in patients with atrial flutter. J Am Coll Cardiol 2000;35:1898–1904.
3. Poty H, Saoudi N, Nair M, Anselme F, Letac B. Radiofrequency catheter ablation of atrial flutter. Further insights into the various types of isthmus block: application to ablation during sinus rhythm. Circulation 1996;94:3204–3213.
4. Shah DC, Jais P, Haissaguerre M, et al. Three-dimensional mapping of the common atrial flutter circuit in the right atrium. Circulation 1997; 96:3904–3912.
5. Gul EE, Boles U, Haseeb S, et al. Gold-tip versus contact-sensing catheter for cavotricuspid isthmus ablation: a comparative study. Turk Kardiyol Dern Ars 2018; 46:464–470.
6. Schmieder S, Ndrepepa G, Dong J, et al. Acute and long-term results of radiofrequency ablation of common atrial flutter and the influence of the right atrial isthmus ablation on the occurrence of atrial fibrillation. Eur Heart J 2003; 24:956–962.
7. Scavee C, Jais P, Hsu LF, et al. Prospective randomised comparison of irrigated-tip and large-tip catheter ablation of cavotricuspid isthmus-dependent atrial flutter. Eur Heart J 2004;25:963–969.
8. Gilligan DM, Zakaib JS, Fuller I, et al. Long-term outcome of patients after successful radiofrequency ablation for typical atrial flutter. Pacing Clin Electrophysiol 2003;26:53–58.
9. Deutsch K, Sledz J, Mazij M, et al. Maximum voltage gradient technique for optimization of ablation for typical atrial flutter with zero-fluoroscopy approach. Medicine (Baltimore) 2017;96:e6939.
10. Bauernfeind T, Kardos A, Foldesi C, Mihalcz A, Abraham P, Szili-Torok T. Assessment of the maximum voltage-guided technique for cavotricuspid isthmus ablation during ongoing atrial flutter. J Interv Card Electrophysiol 2007; 19:195–199.
11. Gula LJ, Redfearn DP, Veenhuyzen GD, et al. Reduction in atrial flutter ablation time by targeting maximum voltage: results of a prospective randomized clinical trial. J Cardiovasc Electrophysiol 2009;20:1108–1112.
12. Subbiah RN, Gula LJ, Krahn AD, et al. Rapid ablation for atrial flutter by targeting maximum voltage-factors associated with short ablation times. J Cardiovasc Electrophysiol 2007;18:612–616.
13. Cheng T, Liu Y, Kongstad O, Hertervig E, Yuan S. Maximum electrogram-guided ablation of cavotricuspid isthmus-dependent atrial flutter. J Electrocardiol 2013;46:670–675.
14. Page RL, Joglar JA, Caldwell MA, et al. 2015 ACC/AHA/HRS Guideline for the Management of Adult Patients With Supraventricular Tachycardia: A Report of the American College of Cardiology/American Heart Association Task Force on Clinical Practice Guidelines and the Heart Rhythm Society. Circulation 2016;133:e506–e574.
15. Tzeis S, Pastromas S, Andrikopoulos G. Ablation of cavotricuspid isthmus-dependent flutter using a mini-electrode-equipped 8-mm ablation catheter: case series. Hellenic Journal of Cardiology 2016;57:53–58.
16. Lewalter T, Weiss C, Spencker S, et al. Gold vs. platinum-iridium tip catheter for cavotricuspid isthmus ablation: the AURUM 8 study. Europace 2011; 13:102–108.
17. Willems S, Weiss C, Ventura R, et al. Catheter ablation of atrial flutter guided by electroanatomic mapping (CARTO): a randomized comparison to the conventional approach. J Cardiovasc Electrophysiol 2000;11:1223–1230.
18. Cabrera JA, Sanchez-Quintana D, Farre J, Rubio JM, Ho SY. The inferior right atrial isthmus: further architectural insights for current and coming ablation technologies. J Cardiovasc Electrophysiol 2005;16:402–408.
19. Sato H, Yagi T, Namekawa A, et al. Efficacy of bundle ablation for cavotricuspid isthmus-dependent atrial flutter: combination of the maximum voltage-guided ablation technique and high-density electro-anatomical mapping. J Interv Card Electrophysiol 2010;28:39–44.
20. Redfearn DP, Skanes AC, Gula LJ, Krahn AD, Yee R, Klein GJ. Cavotricuspid isthmus conduction is dependent on underlying anatomic bundle architecture: observations using a maximum voltage-guided ablation technique. J Cardiovasc Electrophysiol 2006;17:832–838.
21. Caldwell JC, Hobson N, Redfearn D. Voltage-directed cavo-tricuspid isthmus ablation using novel ablation catheter mapping technology. J Innov Card Rhythm Manag 2015;6:1908–1912.
22. Binkowski BJ, Kucejko T, Lagodzinski A, Lubinski A. How to avoid unnecessary RF applications in cavo-tricuspid isthmus: common atrial flutter ablation using 8-mm-tip mini-electrode-equipped catheter. J Interv Card Electrophysiol 2021; 60:109–114.
23. Shah D, Haissaguerre M, Jais P, Takahashi A, Hocini M, Clementy J. High-density mapping of activation through an incomplete isthmus ablation line. Circulation 1999;99:211–215.
24. Caldwell JC, Hobson N, Redfearn D. Importance of anatomy in cavotricuspid isthmus. Europace 2016;18:950.

25. Mol D, Berger WR, Khan M, et al. Additional diagnostic value of mini electrodes in an 8-mm tip in cavotricuspid isthmus ablation. J Atr Fibrillation 2018;11:2082.
26. Takagi T, Miyazaki S, Niida T, et al. Prospective evaluation of a novel catheter equipped with mini electrodes on a 10-mm tip for cavotricuspid isthmus ablation - the efficacy of a mini electrode guided ablation. Int J Cardiol 2017; 240:203–207.
27. Lewalter T, Lickfett L, Weiss C, et al. "Largest amplitude ablation" is the optimal approach for typical atrial flutter ablation: a subanalysis from the AURUM 8 study. J Cardiovasc Electrophysiol 2012;23:479–485.
28. Cano O, Sauri A, Plaza D, et al. Evaluation of a near-zero fluoroscopic approach for catheter ablation in patients with congenital heart disease. J Interv Card Electrophysiol 2019;56:259–269.